Environmental Research 197 (2021) 111059

Contents lists available at ScienceDirect

Environmental Research

journal homepage: www.elsevier.com/locate/envres

Accelerated chromate reduction by tea waste: Comparison of chromate reduction properties between water and ice systems

Tae Uk Han [a], Jungwon Kim [b], Kitae Kim [a,c,*]

[a] Korea Polar Research Institute (KOPRI), Incheon 21990, Republic of Korea
[b] Department of Environmental Sciences and Biotechnology, Hallym University, Chuncheon, Gangwon-do 24252, Republic of Korea
[c] Department of Polar Sciences, University of Science and Technology (UST), Incheon 21990, Republic of Korea

ARTICLE INFO

Keywords:
Waste utilization
Chromate
Ice
Liquid-like layer
Freezing

ABSTRACT

The concentration of chromium (Cr) in natural water and soil environments has gradually increased in recent decades, owing to intensive use of Cr in industry and its subsequent disposal. In this study, we performed a comparison study on chromate (Cr^{6+}) reduction by tea waste (green tea, black tea, red tea, and chamomile) in water (25 °C) and ice (−20 °C) to develop a new strategy for environmental-friendly stabilization of hazardous Cr^{6+} by freezing. This study shows that the freezing process can enhance the reduction of Cr^{6+} by tea waste. The residual Cr^{6+} concentration ratios (C/C_0, where C is the concentration of Cr^{6+} after the reaction (5 h) and C_0 is the initial concentration of Cr^{6+} (20 μM) in the system) by tea wastes in water were in the range of 0.71 (green tea) to 0.92 (chamomile); however, the ratios dramatically decreased under the freezing process (i.e., 0.06 by green tea, 0.13 by black tea, 0.18 by red tea, and 0.08 by chamomile). According to the results obtained from the fluorescent, chromatographic, and spectroscopic analyses, under the freezing process, the enhanced reduction of Cr^{6+} could be explained by the freeze concentration of Cr^{6+}, phenolic components in tea extracts, and protons in small liquid pockets in liquid-like layers (LLLs). In addition, the proposed system can efficiently purify the real Cr^{6+}-containing wastewater (i.e., electroplating wastewater), indicating that the system will be economically feasible in cold regions (i.e., polar regions).

1. Introduction

Large amounts of chromium-containing wastewater are produced primarily due to the intensive use of chromium (Cr) in various industrial fields (e.g., wood preservation, leather tanning, electroplating, and nuclear power plants) (Garg et al., 2007). The Cr concentration in natural water and soil environments has gradually increased in recent decades (López-García et al., 2010).

In the aqueous phase, Cr species exist in trivalent (Cr^{3+}) and hexavalent (Cr^{6+}, chromate) forms (Garg et al., 2007). In the case of metabolism in living organisms, Cr^{3+} is considered an essential element, whereas Cr^{6+} is designated as a hazardous heavy metal ion due to its carcinogenic and mutagenic effects on humans. Therefore, various technologies that are applied to the treatment of Cr-contaminated water and soil are mainly based on the transformation of Cr^{6+} to Cr^{3+} (Mystrioti et al., 2016); this reduction is considered an essential step in the treatment of Cr-contamination because Cr^{3+} is more easily removed than Cr^{6+} by precipitation and adsorption (Kim et al., 2015). Many techniques have been applied for the reduction of Cr^{6+}; they include the methods using nanoparticle (Akika et al., 2020) and biomass (Prabhakaran et al., 2009; Cherdchoo et al., 2019) and so on. In one study, the use of photocatalysts, such as TiO_2 and SnO_2, were applied for the stabilization of toxic Cr^{6+}; however, a disadvantage is that these catalysts are activated by the UV irradiation (Akika et al., 2020). Therefore, there has been an increasing interest in finding new photocatalysts (i.e., Cu-doped $ZnAl_2O_4$ and La_2NiO_4/TiO_2) for Cr^{6+} reduction, which are activated in the visible region (Lahmar and Benamira 2017; Akika et al., 2020) so as to establish an economical and environmentally-friendly technique for Cr^{6+} reduction. In this regard, tea wastes, which are solid particles generated after brewing tea, can be suitable biomass for Cr^{6+} reduction because polyphenol extracts in tea waste can serve as electron donors in the reduction reaction (Prabhakaran et al., 2009; Cherdchoo et al., 2019). The use of waste biomass (i.e., tea wastes) for Cr^{6+} reduction is a promising strategy in terms of environmentally friendly waste management and utilization strategies. Previous studies (Prabhakaran et al., 2009; Cherdchoo et al., 2019) reported that Cr^{6+}

* Corresponding author. Korea Polar Research Institute (KOPRI), Incheon, 21990, Republic of Korea.
E-mail address: ktkim@kopri.re.kr (K. Kim).

https://doi.org/10.1016/j.envres.2021.111059
Received 30 December 2020; Received in revised form 11 March 2021; Accepted 17 March 2021
Available online 22 March 2021
0013-9351/

reduction could be achieved using tea wastes and coffee dust because of the electron-donor properties of their polyphenol extracts. However, the application of large amounts of tea waste and coffee dust can be disadvantageous as a purification method because an additional treatment process is required to oxidize the large amounts of polyphenols.

According to the Arrhenius equation, chemical reactions slow down as the reaction temperature decreases. However, it has recently been reported that the freezing process can accelerate some chemical reactions. For example, the reaction efficiencies of (1) the oxidation of nitrite (NO_2^-) by dissolved oxygen (Takenaka et al., 1992), (2) the oxidation of organic pollutants by periodate (IO_4^-) (Choi et al., 2018) and peroxymonosulfate (Le et al., 2020), and (3) the reduction of heavy metal ion (i.e., Cr^{6+}) by hydrogen peroxide (H_2O_2) (Kim et al., 2015), phenolic compounds (Ju et al., 2017), nitrite (Kim et al., 2017), biochar (Han et al., 2020), hydrogen sulfide (Nguyen et al., 2020), and ferrous ions (Nguyen et al., 2021) were dramatically accelerated during the freezing process. This can be primarily ascribed to the freeze concentration effect (O˙Concubhair et al., 2012). When an aqueous solution is frozen, the solutes in the solution concentrate in small liquid pockets (i.e., liquid-like layers; LLLs), where increased collision efficiency between the solutes results in an enhanced rate of chemical reactions. Furthermore, protons are also accumulated in LLLs by freezing, which results in a decrease in the pH of the reaction system (Heger et al., 2006). Since Cr^{6+} reduction is favored at low pH, changing the properties of the reaction system by freezing may enhance the Cr^{6+} reduction by tea wastes (Archundia et al., 1993).

In terms of practical application, tea waste/freezing system proposed in this paper will have advantages compared to previous literature. The use of tea wastes for water purification meets global concept of solid waste management and utilization (i.e., 6R: reduce, reuse, recycle, redesign, remanufacture, and recover) (Siddiqui et al., 2020). This system does not require chemicals (i.e., H_2O_2, phenolic compounds, nitrite, hydrogen sulfide, and ferrous ions) and synthesized materials (i.e., biochar) for Cr^{6+} reduction because natural tea extracts contain polyphenols, which can act as reducing agents. In addition, due to the freeze concentration effect, lower quantities of reducing agents (i.e., tea wastes) in the ice phase will be required for Cr^{6+} reduction compared to that in the water phase. Therefore, we conducted the comparison study on Cr^{6+} reduction by tea wastes in water and ice phase to investigate detailed reduction properties, which has not been discussed in prior literature.

To investigate the potential of the freeze effect to facilitate Cr^{6+} reduction, in this study, we conducted a comparison of Cr^{6+} reduction by tea wastes in water (25 °C) and ice (−20 °C). Four different types of tea were employed in this study (green tea, black tea, red tea, and chamomile). The reduction efficiencies of Cr^{6+} using tea wastes were investigated in water and ice under various conditions, and the main reaction pathway in ice was investigated using spectroscopic and chromatographic analyses. By understanding the detailed reduction properties of Cr^{6+} in the ice phase, this study can provide fundamental data for the actual commercialization of the tea waste/freezing system for Cr^{6+} reduction.

2. Materials and methods

2.1. Sample preparation and chemicals

Four types of tea (green tea, black tea, red tea, and chamomile) were infused at 85 °C (5 min). For chromate reduction tests, 100 mg of waste tea residues were collected, rinsed twice with 1 L of ultrapure deionized (DI) water at 25 °C (Milli-Q Direct 16 System, Merck-Millipore, Darmstadt, Germany), and then air-dried at 50 °C for 48 h. The dried samples were cryo-milled with liquid nitrogen and sieved to particle sizes below 63 μm. Tea wastes before and after cryo-milling are presented in the supplementary information (Fig. S1). Industrial chromate-polluted wastewater was also prepared from an electroplating plant in the Republic of Korea for the feasibility test of the tea waste/freezing system. The detailed chemical composition of the chromate-contaminated wastewater is listed in the supplementary information (Table S1) (Kim et al., 2015).

All chemicals were prepared and used in this study without further purification, and include the following: sodium dichromate dehydrate ($Na_2Cr_2O_7{\cdot}2H_2O$, chromate (Cr^{6+}), ≥99.5%, Sigma-Aldrich) for chromate reduction tests in water and ice, 1,5-diphenylcarbazide ($C_6H_5NHNHCONHNHC_6H_5$, DPC, ≥ 99.95%, Sigma-Aldrich), sulfuric acid (H_2SO_4, ≥96.0%, Kanto Chemical), and acetone (CH_3COCH_3, ≥99.5%, Kanto Chemical) for determining the residual concentration of chromate by the DPC method after reaction (Ju et al., 2017), cresol red ($C_{21}H_{18}O_5S$, CR, ≥ 95.0%, Sigma-Aldrich) for estimating the pH value of LLLs, and methanol (CH_3OH, liquid chromatograph-mass spectrometry (LC-MS) grade, Supelco Co.), formic acid (CH_2O_2, LC-MS grade, Supleco Co.), and acetonitrile (CH_3CN, high-performance LC (HPLC) grade, J.T. Baker) for LC-MS analysis.

2.2. Experimental procedure

An aliquot of chromate (2 mM, 2 mL) and the desired amount of tea waste (0.02 g) were added to the DI water in a beaker (198 mL) to yield the desired initial concentration (i.e., [Cr^{6+}] = 20 μM and [tea waste] = 0.1 g/L). The initial pH of the solution (200 mL) was adjusted to the desired value (pH = 3.5) using perchloric acid ($HClO_4$, 1 M), and sodium hydroxide (NaOH, 1 M) solution. For the comparison test of chromate reduction in water and ice, conical tubes (Falcon, 15 mL) containing the adjusted solution (10 mL) were placed in a laboratory-made holder installed inside the pre-adjusted ethanol baths (i.e., 25 °C for water, and −20 °C for ice). The reaction time was measured from the moment when the conical tube was placed in the ethanol bath. The reactions were allowed to run for fixed time intervals (0.5, 1, 2, 3, 4, and 5 h), after which the samples were collected and thawed in warm water (45 °C) in a beaker; samples were filtered using a syringe filter (0.45 μm) to remove tea waste particles, and then analyzed immediately. Experiments were performed at least twice to confirm the reproducibility of the data.

2.3. Analytical methods

2.3.1. Chemical analyses

The concentration of Cr^{6+} was spectrophotometrically analyzed by measuring the absorbance at 540 nm (a purple complex of Cr^{6+} with DPC reagent) (Ju et al., 2017). The concentration of total [Cr] in the solution after the reaction was analyzed using inductively coupled plasma-optical emission spectroscopy (ICP-OES; iCAP 7600 Duo, Thermo Fisher Co.). The adsorptive removal concentration of [Cr] by tea waste was calculated as the difference between the total [Cr] and [Cr^{6+}].

The estimation of the pH of the LLL in frozen solution was measured using a UV/vis spectrometer coupled with an integrating sphere (Carry 5000, Agilent Technologies); the absorbance of cresol red (CR) was used as a pH indicator. To this end, the cuvette containing aqueous solution frozen at −20 °C in the ice bath for 1 h, and UV–vis spectra of CR in the frozen solution were measured without the melting process. As reported elsewhere, a different maximum absorption wavelength is reported depending on the pH value (Heger et al., 2006).

The concentration of total organic carbon (TOC) was measured using a TOC analyzer (TOC-V_{CSH}, Shimadzu Co.) equipped with a nondispersive infrared sensor (NDIR) to compare the efficiency of redox conversion between Cr^{6+} and extracts derived from tea wastes in water and ice. In addition, a fluorescent excitation-emission measurement was performed using a fluorescence spectrophotometer (FLS-1000, Edinburgh Instrument Ltd.) to determine the qualitative characterization of extracts before and after the reaction in water and ice systems, in accordance with established procedures (Han et al., 2020).

The instrument used for chemical analysis consisted of an Ultra-high performance liquid chromatography (UHPLC; Vanquish, Thermo Fisher

Co.) coupled with a diode array detector (DAD), and an Orbitrap mass spectrometer (MS; Q Exactive Focus, Thermo Fisher Co.). A C18 column (Hypersil GOLD VANQUISH aQ, 100 mm × 2.1 mm, 1.9 μm; Thermo Fisher Co.) was used at a flow rate of 0.5 mL/min that consisted of two mobile phases (eluent A: 0.1% (V/V) formic acid in water, and eluent B: 0.1% (V/V) formic acid in acetonitrile). The DAD was set at 270 nm for real-time monitoring of the peak intensity, and MS data was simultaneously acquired using positive and negative electrospray ionization (ESI) modes. The detailed LC-DAD-MS operating conditions are given in the supplementary information (Table S2).

Fourier transform infrared spectroscopy (FTIR; NICOLET iN10 MX, Thermo Fisher Co.) analysis was also conducted in the attenuated total reflection (ATR) mode to understand the difference in the adsorptive behaviors of tea wastes.

2.3.2. Microscopic analyses

To verify the freeze concentration behavior of Cr^{6+} and tea extracts during the freezing process, we performed two microscopic analyses of the frozen solution ($[Cr^{6+}] = 1$ mM, [chamomile] = 5.0 g/L, and $pH_i = 3.5$). Confocal Raman spectroscopy (Renishaw inVia Qontor) was used to obtain the frozen solution's optical image, and its spatial distribution based on the peak intensity at 900 cm^{-1} for Cr^{6+} was obtained using a monochromatic laser ($\lambda = 532$ nm). In addition, confocal fluorescence images were obtained using a confocal laser scanning microscope (LSM 800 Exciter, Carl-Zeiss) under a filter excitation wavelength between 335–383 nm, and emission wavelength of 420–470 nm with a Si laser. All microscopic analyses of the frozen solution were carried out on a temperature-controlled cryostage (THMS600, Linkam Scientific). To this end, the temperature of the aqueous solution (one droplet of the aqueous solution) was reduced from 20 °C to −20 °C at a freezing rate of −2 °C/min.

3. Results and discussion

3.1. Reduction of chromate by tea wastes in water and ice

Fig. 1 reveals the concentration ratios (C/C_0) of total Cr and Cr^{6+} after 5 h reaction in the system, where C_0 is the initial concentration of total Cr and Cr^{6+} (i.e., $C_0 = [Cr^{6+}]_i = [\text{total Cr}]_i = 20$ μM), and C is the residual concentration of total Cr and Cr^{6+} in the system. Although the change of total Cr concentration in both of the phases was negligible (i.e., $C_0/C = 1$ in the absence of tea wastes, 0.92 (green tea), 0.95 (black tea), 0.89 (red tea), and 0.97 (chamomile) in the ice phase), the concentration of Cr^{6+} in ice significantly decreased in the presence of tea wastes (i.e., $C_0/C = 0.84$ in the absence of tea wastes, 0.06 (green tea), 0.13 (black tea), 0.18 (red tea), and 0.08 (chamomile)). Therefore, this confirms that the enhanced reduction of Cr^{6+} in this system is mainly due to the redox reaction of Cr^{6+} to Cr^{3+} (not the adsorption of Cr^{6+} on the surface of tea wastes) by freezing in the presence of tea wastes.

Fig. 2 shows the reduction kinetics of Cr^{6+} by different tea wastes depending on the reaction time in water and ice, where C_0 is the initial concentration of Cr^{6+} (i.e., $C_0 = [Cr^{6+}]_i = 20$ μM), and C is the residual concentration of Cr^{6+} in the system. In the water phase, Cr^{6+} was barely converted to Cr^{3+} in the absence of tea wastes; however, the concentration of Cr^{6+} gradually decreased in the presence of tea wastes (Fig. 2). Notably, the reduction capacities of Cr^{6+} by tea wastes were dramatically enhanced under the freezing process. Furthermore, in the absence of tea wastes, the reduction of Cr^{6+} still proceeded in the ice phase to a small degree ($C/C_0 = 0.84 \pm 0.02$); this implies that the pH in the system was lowered under the freezing process, because Cr^{6+} can be thermodynamically and pH-dependently reduced *via* the proton-mediated pathway (i.e., $4HCr^{6+}O_4^- + 16H^+ \rightarrow 4Cr^{3+} + 3O_2 + 10H_2O$; $E_0 = 0.15$ V_{NHE}) (Kim et al., 2015). However, the reduction efficiency in the absence of tea waste was relatively lower than that of when tea wastes were present. Therefore, the enhanced reduction of Cr^{6+} can be achieved in the presence of both tea wastes and the freezing process.

The enhanced reduction of Cr^{6+} by tea wastes in the ice phase might be due to the concentration of Cr^{6+} and protons (H^+), as well as organic components extracted from tea wastes, which can act as electron donors (reductants) (O'Concubhair et al., 2012; Ju et al., 2017; Han et al., 2020). To verify the accumulation of protons in LLLs (Figs. S2 and 3), changes in the UV–vis absorption spectra of CR were monitored before and after freezing (Heger et al., 2006; Han et al., 2020; Nguyen et al., 2021). The results showed that the absorption band at 518 nm (doubly protonated CR) was newly observed along with the 434 nm band (singly protonated CR) in the frozen solution. Fig. S2 shows the UV–vis absorption spectra of CR in the absence of tea wastes, and the calculated pH of the LLLs was approximately 1.69. Therefore, it confirms that Cr^{6+} reduction even in the absence of tea wastes in the ice phase was due to the proton-mediated reduction in the ice phase (Fig. 2b). Furthermore, the pH of the LLLs also decreased in the presence of tea wastes (i.e., the calculated pH values of the frozen solution containing tea wastes were 1.48 (green tea), 1.50 (black tea), 1.67 (red tea), and 1.71 (chamomile), respectively). It indicates that the accelerated reduction of Cr^{6+} to Cr^{3+} could account for the accumulation of Cr^{6+} and protons, as well as organic components extracted from tea wastes in LLLs.

As shown in Table 1, after 5 h of reaction in the presence of tea wastes, the residual concentrations of TOC in ice were much lower than those in water. This indicates that the enhanced redox reaction between Cr^{6+} and organic components in LLLs (Han et al., 2020) proceeds under the freezing process. To further clarify the enhanced Cr^{6+} reduction pathway, the change in the excitation-emission matrix (EEM) was investigated before and after the reaction, in both water and ice conditions (Fig. 4). According to the EEM regions, the qualitative properties of organic components extracted from tea wastes can be assigned (i.e., regions 1 and 2: aromatic protein, region 3: fulvic acid-like matter, region 4: soluble microbial by-product-like matter, and region 5: humic acid-like matter) (Chen et al., 2003; Li et al., 2021). Although there was a difference in fluorescence intensity depending on the TOC value (Table 1), the organic components of green, black, and red tea were characterized by aromatic proteins and soluble microbial by-product-like compounds. Meanwhile, the extracted components from the chamomile tea were mainly characterized by humic acid-like compounds with fulvic acid-like matter. As shown in Fig. 4, the water phase's fluorescence intensities were slightly lowered; however, these were significantly reduced in the ice phase. Therefore, the combined results presented in Table 1 and Fig. 4 confirm that the enhanced redox reaction between Cr^{6+} and organic components in ice is the main reason for the

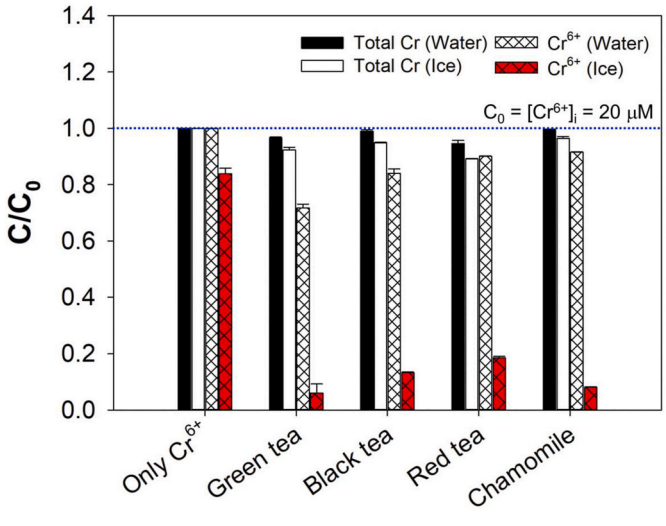

Fig. 1. Residual ratios of total Cr and Cr^{6+} in water (25 °C) and ice (−20 °C) in the system. Experimental conditions: [tea waste] = 0.1 g/L, $pH_i = 3.5$, reaction time = 5 h, and freezing temperature = −20 °C.

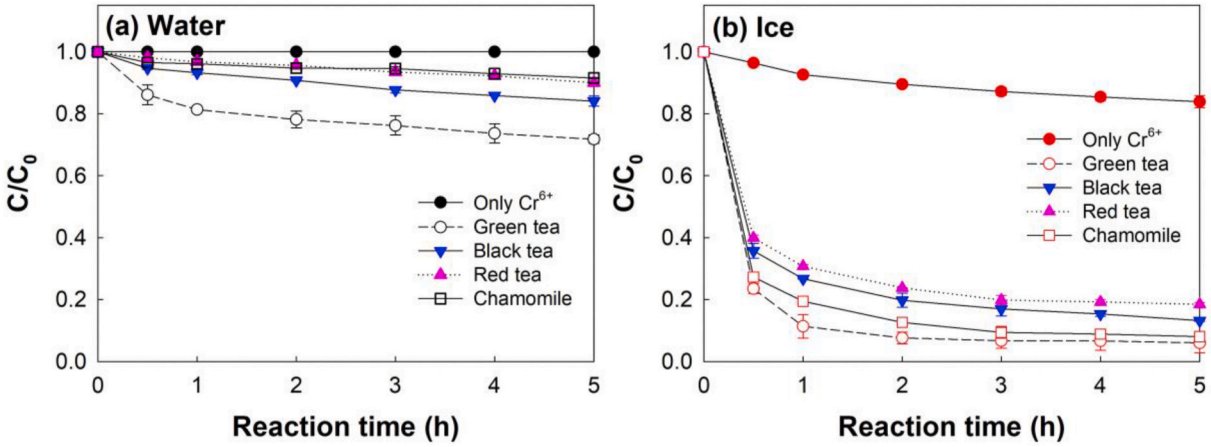

Fig. 2. Reduction of Cr^{6+} in the presence of tea waste in (a) water (25 °C) and (b) ice (−20 °C), where C is the residual concentration of Cr^{6+} in the system. Experimental conditions: $C_0 = [Cr^{6+}]_i = 20$ μM, [tea waste] = 0.1 g/L, $pH_i = 3.5$, and freezing temperature = −20 °C.

accelerated Cr^{6+} reduction.

LC chromatograms obtained at 270 nm before and after 5 h of reaction are shown in Fig. 5, and Table S3 lists the peak areas for each component. Each peak was identified by Compound Discoverer software based on exact masses and the fragmentation spectra of MS data (Lin et al., 2008; Lin and Harnly 2010; Cerrato et al., 2020). As shown in Fig. 5a and b, both green and black tea extracts had large amounts of

Table 1
Residual concentration of Total Organic Carbon (TOC, mg C/L) in water and ice after 5 h reaction.

mg C/L	Green tea	Black tea	Red tea	Chamomile
$[TOC]_{initial}$	8.312 ± 0.053	4.504 ± 0.016	3.501 ± 0.072	7.807 ± 0.010
$[TOC]_{water}$	8.094 ± 0.021	4.296 ± 0.051	3.278 ± 0.038	7.696 ± 0.018
$[TOC]_{ice}$	5.846 ± 0.023	3.143 ± 0.036	2.260 ± 0.031	6.045 ± 0.010

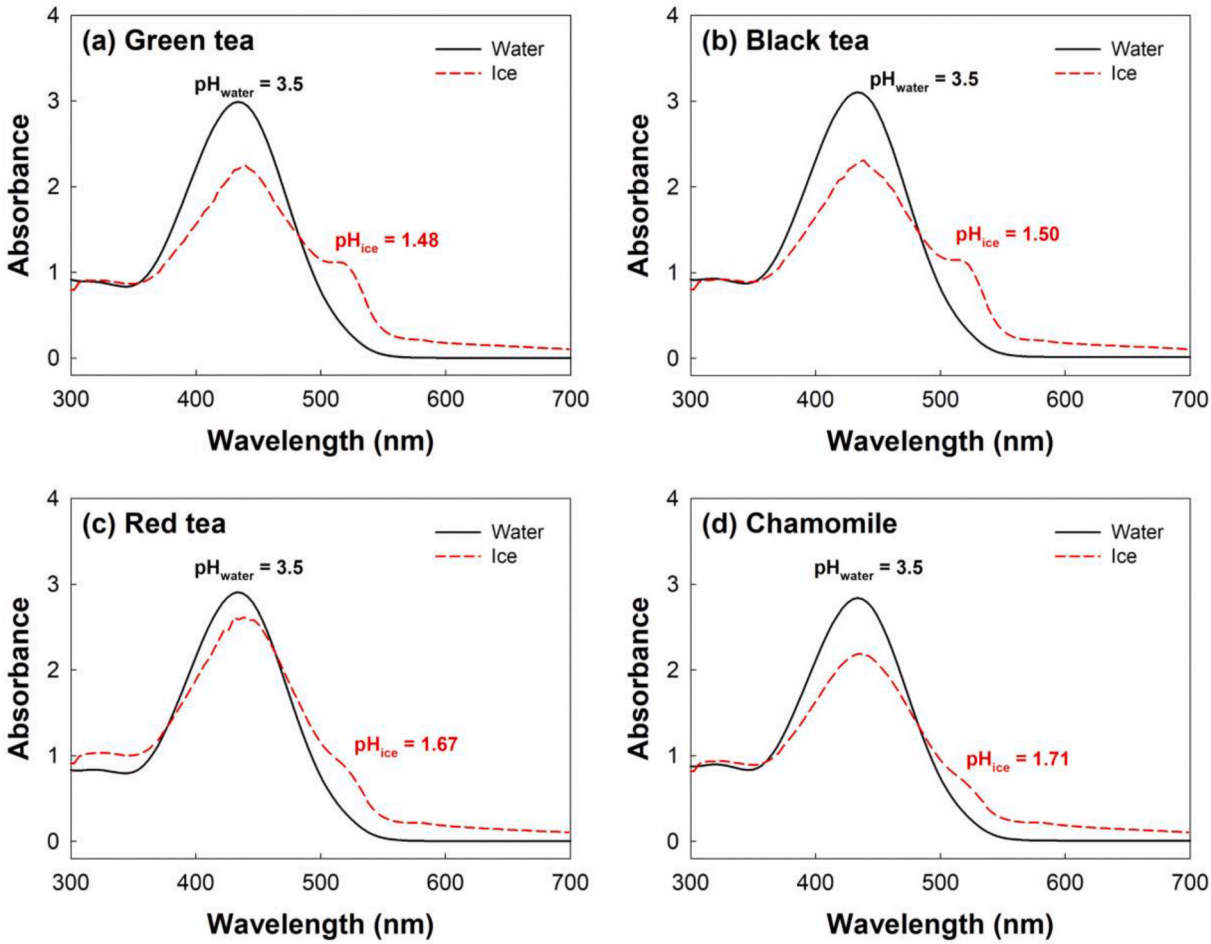

Fig. 3. Changes of UV–vis absorption spectra of cresol red (CR) before and after freezing under the experimental conditions $[Cr^{6+}]_i = 20$ μM, $pH_i = 3.5$, freezing temperature = −20 °C, and freezing time = 1 h. (For interpretation of the references to colour in this figure legend, the reader is referred to the Web version of this article.)

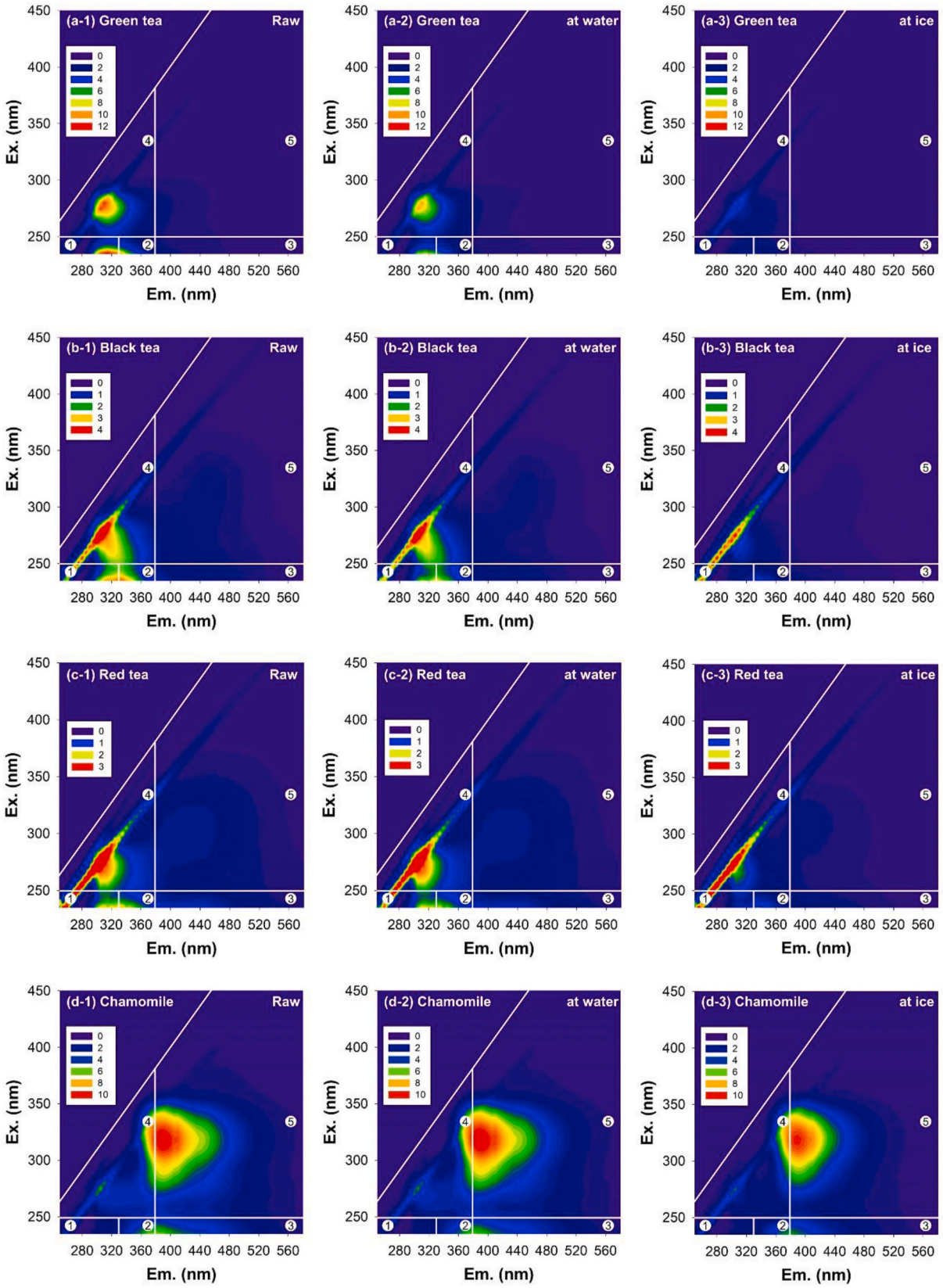

Fig. 4. Excitation-emission matrix (EEM) of the tea extracts before and after reaction. Experimental conditions: $C_0 = [Cr^{6+}]_i = 20$ μM, [tea waste] = 0.1 g/L, $pH_i = 3.5$, and freezing temperature = −20 °C.

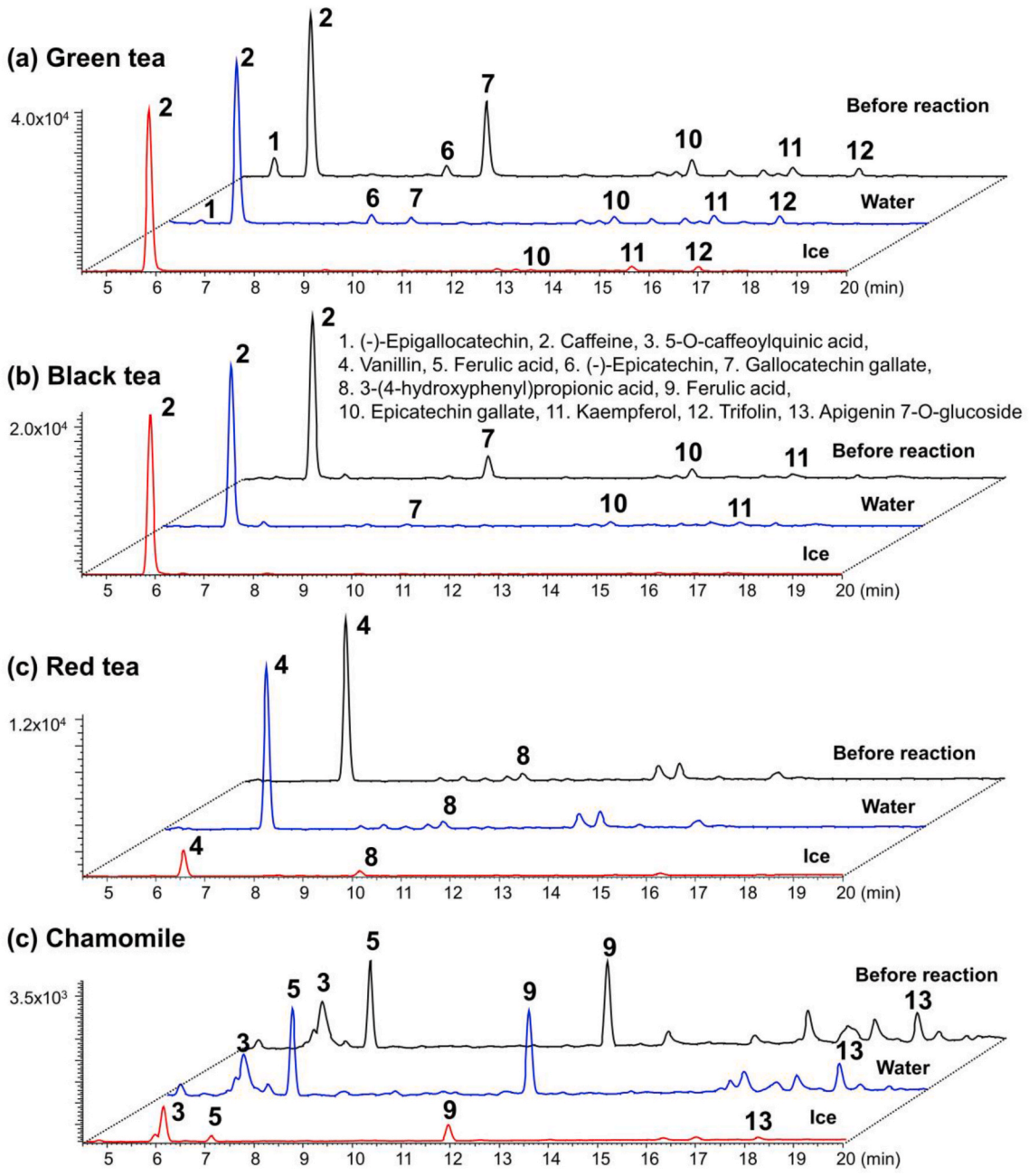

Fig. 5. LC-DAD chromatogram (270 nm) of the extracts derived from tea wastes after 6 h of reaction in water and ice.

caffeine (peak #2), which is known to be the main component of green and black tea (Lin et al., 2003); however, no changes in peak area were observed. This means that caffeine does not participate in Cr^{6+} reduction. Meanwhile, the peak areas of other phenolic components, such as gallocatechin gallate (peak #7), epicatechin gallate (peak #10), and trifolin (peak #11) were reduced in both the water and ice phases. Notably, the peak areas of these components decreased more in the ice phase (Table S3) compared with those detected in the water phase. Although the accelerated reduction of Cr^{6+} by red tea and chamomile was also observed, it could be seen that the main electron donors for Cr^{6+} were different from those of green and black tea (Fig. 5c and d). Red tea and chamomile are caffeine-free teas (Stander et al., 2019; Cleverdon et al., 2018); as expected, caffeine was not detected in the extracts of either. Furthermore, it was observed that the extracts of red tea and chamomile consisted of different types of phenolic components (i.e., vanillin (peak #4) and 3-(4-hydroxyphenyl) propionic acid (peak # 8) in the case of red tea, and 5-O-caffeoylquinic acid (peak #3), ferulic acids (peak #5 and #9), and apigenin 7-O-glucoside (#13) in the case of chamomile). As shown in Fig. 5c and d, the changes in the peak areas were negligible in water; however, vanillin in red tea extracts, and ferulic acid in chamomile extracts among phenolic components were significantly reduced in ice. Therefore, this finding confirms that phenolic components of tea extracts act as electron donors for Cr^{6+} reduction (Prabhakaran et al., 2009; Han et al., 2020), and that the freezing process enhances redox conversion between Cr^{6+} and phenolic components. In addition, it should be noted that the Cr^{6+} reduction capacities by tea wastes were different, because organic constituents extracted from different tea wastes have different ligands properties to form a precursor (i.e., chromate ester intermediate) for the reduction of Cr^{6+} to Cr^{3+} (Han et al., 2020).

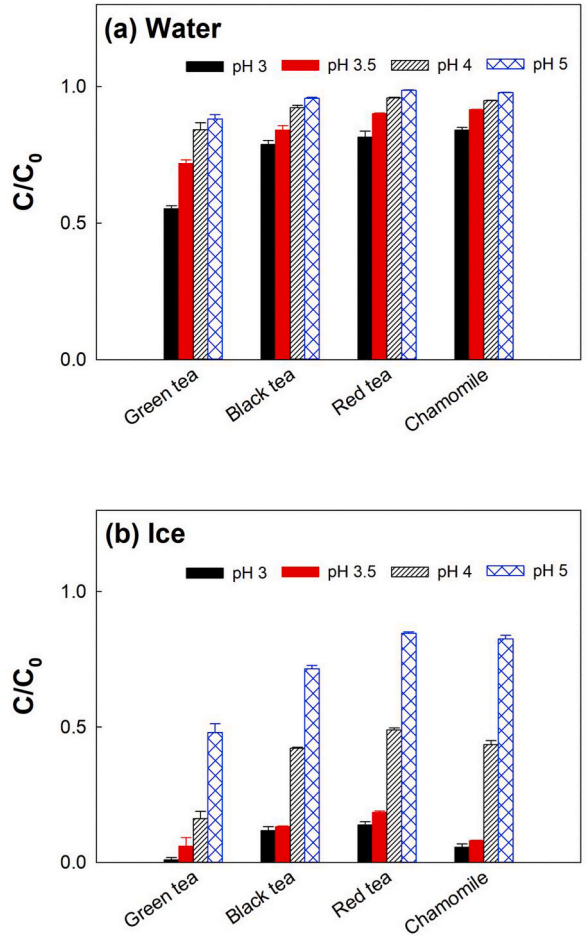

Fig. 6. Effect of pH on the reduction of Cr^{6+} by tea wastes in (a) water and (b) ice. Experimental conditions: $C_0 = [Cr^{6+}]_i = 20$ μM, [tea waste] = 0.1 g/L, freezing temperature = −20 °C, and reaction time = 5h.

3.2. Effect of initial pH and tea waste dosage on chromate reduction

This study also investigated the effects of initial pH, and the concentration of tea waste on Cr^{6+} reduction and removal. Fig. 6 shows the pH dependent Cr^{6+} reduction by tea waste in water and ice. The Cr^{6+} reduction capacity increased in both phases as initial pH value decreased, indicating that the pH value of the system significantly influences the Cr^{6+} reduction (Kim et al., 2015; Ju et al., 2017; Nguyen et al., 2020, 2021). Notably, under lower pH conditions, the reduction capacities of Cr^{6+} in the ice phase were dramatically enhanced in comparison with those in the water phase. Furthermore, the reduction of Cr^{6+} was more favorable at lower pH values under the same concentration of tea wastes (Archundia et al., 1993). Therefore, the results confirm that pH of the system is the crucial factor in Cr^{6+} reduction (Xu et al., 2019), and the accumulation of protons in LLLs is one of the main factors for enhancing Cr^{6+} reduction during the freezing process.

To investigate the effect of tea waste concentration on Cr^{6+} reduction and removal, the residual concentrations of Cr^{6+} and total Cr were also measured as a function of tea waste dosage, in the range of 0.1–0.5 g/L (Fig. 7). In both phases, the residual concentration of Cr^{6+} decreased as the tea waste dosage increased (Fig. 7a). It should be noted that the residual concentrations of Cr^{6+} in the water at 0.5 g/L of tea waste was higher than those in ice at 0.1 g/L of tea waste; this indicates that there are more tea extracts (i.e., phenolic compounds) in LLLs, as the aqueous system was frozen at least five times. Therefore, the concentration of electron donors increases in the reaction system, resulting in enhanced reduction of Cr^{6+}. These combined results (Figs. 6 and 7a) imply that proton and phenolic components will accumulate in LLLs.

The removal (sorption) of Cr^{6+} proceeds *via* a two-step process: (1) Cr^{6+} is transformed to Cr^{3+}, and (2) Cr^{3+} is complexed on the absorbent surface (Kim et al., 2015; Li et al., 2017). As expected, the adsorptive capacities of Cr^{6+} in both phases followed proportionally as tea waste concentration increased (Fig. 7b). This is due to the increase in the total number of adsorption sites, especially O-containing functional groups (Chen et al., 2011; Han et al., 2020). A higher adsorptive removal efficiency was observed among wastes from red tea, and enhanced in the frozen solution. Meanwhile, the enhancing capacities of other tea wastes in ice were negligible. This can be explained by the differences in the functional groups on the surface (Fig. S3, FT-IR spectra of tea wastes in the supplementary information). It has been reported that Cr^{3+} complexation on the surface is not favored in the presence of aliphatic hydrocarbons (Liu et al., 2015). As shown in Fig. S3, red tea contains smaller amounts of aliphatic hydrocarbons on the surface compared to other types of tea waste. Therefore, these results suggest that reducing the toxicity of Cr^{6+} *via* transformation to Cr^{3+} by tea wastes could be possible through the freezing process (i.e., an essential step for Cr^{6+} removal by adsorbents); however, the functional groups of a bio-adsorbent should be considered to enhance the removal of chromium simultaneously.

3.3. Freeze concentration of chromate and environmentally-friendly reductants in LLLs

To further confirm the freeze concentration of Cr^{6+} and tea extracts, the distribution of Cr^{6+} and tea extracts in the ice phase (Fig. 8) were monitored in-situ using confocal Raman spectroscopy, and confocal laser scanning microscopy under the initial conditions of $[Cr^{6+}]_i = 1$ mM, [chamomile]$_i$ = 5.0 g/L, and $pH_i = 3.5$. According to previous studies, the specific Raman peak of Cr^{6+} is in the range of 800–1000 cm^{-1} based on the concentration of Cr^{6+} and pH (Kim et al., 2020). As shown in Fig. 8a, we selected two points, one that is representative of an ice crystal (site marked with a black circle), and the other representative of LLLs (site marked with a red circle); this revealed that the Raman peak intensity of Cr^{6+} dramatically increased at LLLs (Fig. 8b). In addition, the distribution of Cr^{6+} in the square region (Fig. 8c) in the frozen solution was monitored at 900 cm^{-1} (Fig. 8d), reconfirming that Cr^{6+} significantly accumulated at LLLs by exclusion from ice crystals.

Fig. 8e and f shows confocal microscopy images that visualize the accumulation of the extracts in LLLs (Lee et al., 2019). In particular, the merged image (Fig. 8f, an overlap image of the fluorescence with DIC) clearly shows that the enhanced reduction of Cr^{6+} should be accounted for in the freeze concentration of Cr^{6+}, as well as the concentrations of protons and tea extracts (especially phenolic components).

3.4. Practical application of tea waste/freezing system in chromate-containing wastewater

To check the feasibility of the tea waste/freezing system for the purification of real Cr^{6+} containing wastewater, the residual concentrations of Cr^{6+} in electroplating wastewater before and after 5 h of reaction were compared to those in artificial Cr^{6+} wastewater (Fig. 9a). The enhanced reduction of Cr^{6+} in electroplating wastewater was also observed in the ice phase for all tea wastes. Notably, although the electroplating wastewater contained other elements (Table S1), the efficiencies of Cr^{6+} reduction were comparable with those observed with the artificial Cr^{6+} wastewater. This observation indicates that other elements do not affect the acceleration of freeze-induced reduction of Cr^{6+} by tea wastes. Furthermore, the accelerated reduction of Cr^{6+} in electroplating wastewater by raw tea wastes was also feasible in the ice phase (Fig. 9b), although, the reduction capacities were slightly lower than those by cryo-milled tea wastes due to the effects of particle size. Previous study has established that the extraction capacity of organic components from the samples (i.e., tea wastes) with small sized particles

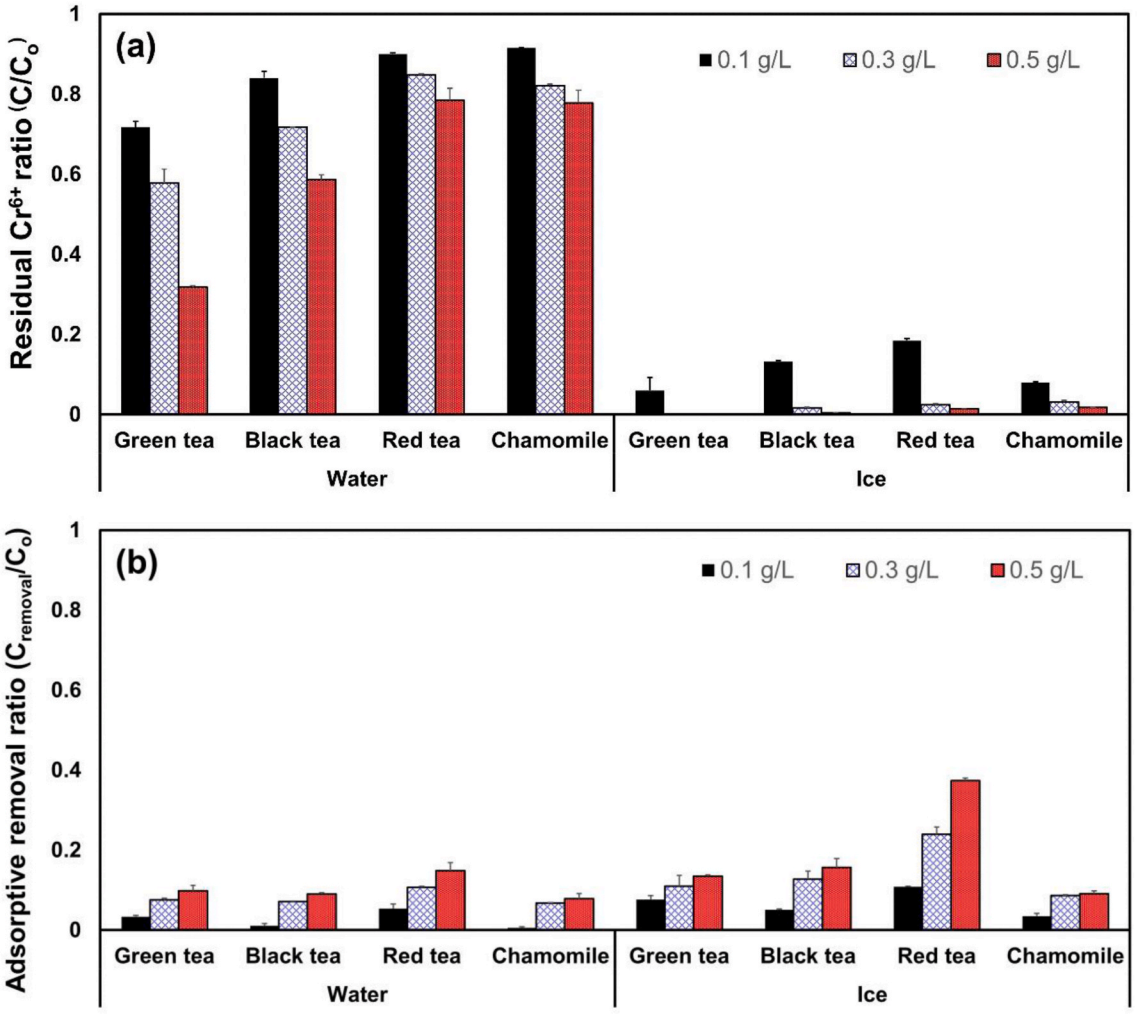

Fig. 7. Effect of dosage of tea waste on (a) the reduction of Cr^{6+} by tea wastes, and (b) the adsorptive removal of Cr by tea wastes in water and ice, where C_0 and C are the initial and residual concentration of Cr^{6+} in the system and $C_{removal}$ is the adsorptive removal concentration of Cr^{6+} by the tea wastes. Experimental conditions: $C_0 = [Cr^{6+}]_i = 20$ μM, $pH_i = 3.5$, freezing temperature = −20 °C, and reaction time = 5h.

is higher than that with large size particles (Sari and Velioglu, 2011).

The proposed system (tea waste/freezing method) has utility as the first step for Cr^{6+} removal; the use of tea wastes could supplant the use of large amounts of chemicals, such as sulfur compounds and iron salts. However, a drawback of the proposed system is that it needs external energy for freezing. Therefore, a variety of methods are necessary to address the technical and economic issues to ensure the successful application of the proposed system. The applicability of the proposed system will be relatively high in regions where low temperatures (below −10 °C) are maintained, such as polar regions, high latitudes, and mid-latitudes (Le et al., 2020).

4. Conclusions

In this study, we developed a new Cr^{6+} reduction method using tea wastes and freezing process. Using tea waste biomass for Cr^{6+} reduction is a promising strategy in addressing recovery, one of the basic concepts of waste management (i.e., the 6 Rs: reduce, reuse, recycle, redesign, remanufacture, and recover). To this regard, the results showed that the freezing process could achieve accelerated Cr^{6+} reduction by tea wastes via the freeze concentration effect. When solutions containing Cr^{6+} and tea wastes were frozen, the solutes (Cr^{6+} and tea extracts) with protons were dramatically accumulated in LLLs, wherein the redox conversion efficiency between Cr^{6+} and polyphenols in tea extracts increased. Among tea wastes, red tea has smaller quantities of aliphatic hydrocarbon functional groups compared to others, a characteristic that was found to be more favorable for reducing total Cr; additionally, the adsorptive capacity was enhanced in ice as the dosage of red tea increased due to the increase in adsorption sites. The results indicate that the properties of biomass surface functional groups should be checked when simultaneously enhanced reduction and adsorption are achieved. However, under red tea treatment, the adsorptive capacity was very low (adsorptive removal ratio of 0.1 g/L of red tea, $C/C_0 = 0.11$), indicating that the proposed system will be more suitable for the reduction of Cr^{6+}. Notably, the real Cr^{6+}-contaminated wastewater, which contained large amounts of other metal ions, was successfully treated by the freezing process, indicating that the freezing process with tea waste could be feasible for the stabilization of Cr^{6+}.

Declaration of competing interest

The authors declare that they have no known competing financial interests or personal relationships that could have appeared to influence the work reported in this paper.

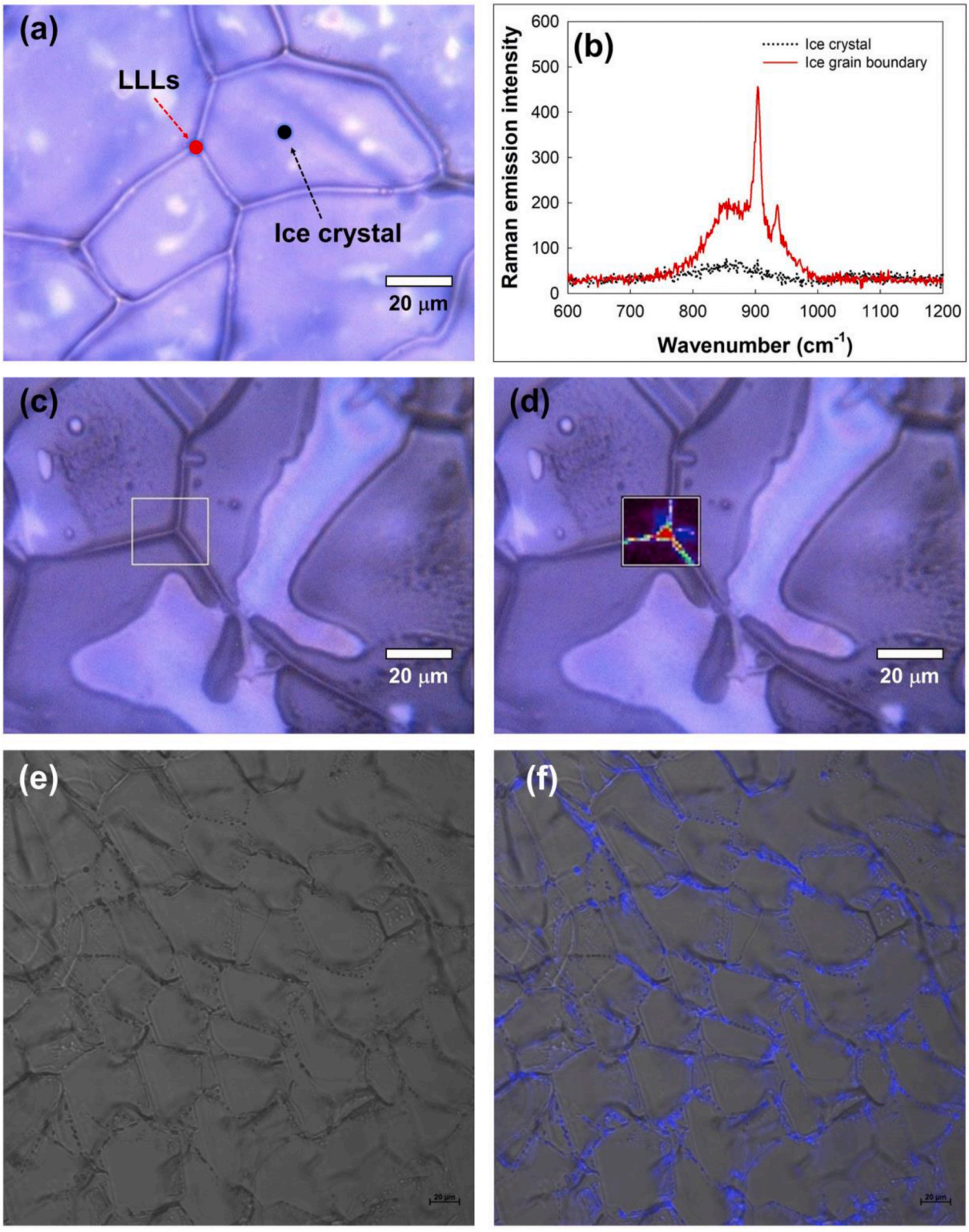

Fig. 8. (a and b) Optical image of the frozen Cr^{6+} with chamomile solution and its Raman spectra in LLLs (site marked with red circle in Fig. 7a) and ice crystal (site marked with black circle in Fig. 7b), (c and d) optical image of the frozen Cr^{6+} with chamomile solution and its spatial distribution based on the peak intensity at 900 cm^{-1}, (e–f) confocal microscopy image of the frozen Cr^{6+} with chamomile, and merged image obtained using the DIC image and fluorescence image of chamomile extracts under the conditions of $C_0 = [Cr^{6+}]_i = 1$ mM, $[chamomile]_i = 5.0$ g/L, and $pH_i = 3.5$. (For interpretation of the references to colour in this figure legend, the reader is referred to the Web version of this article.)

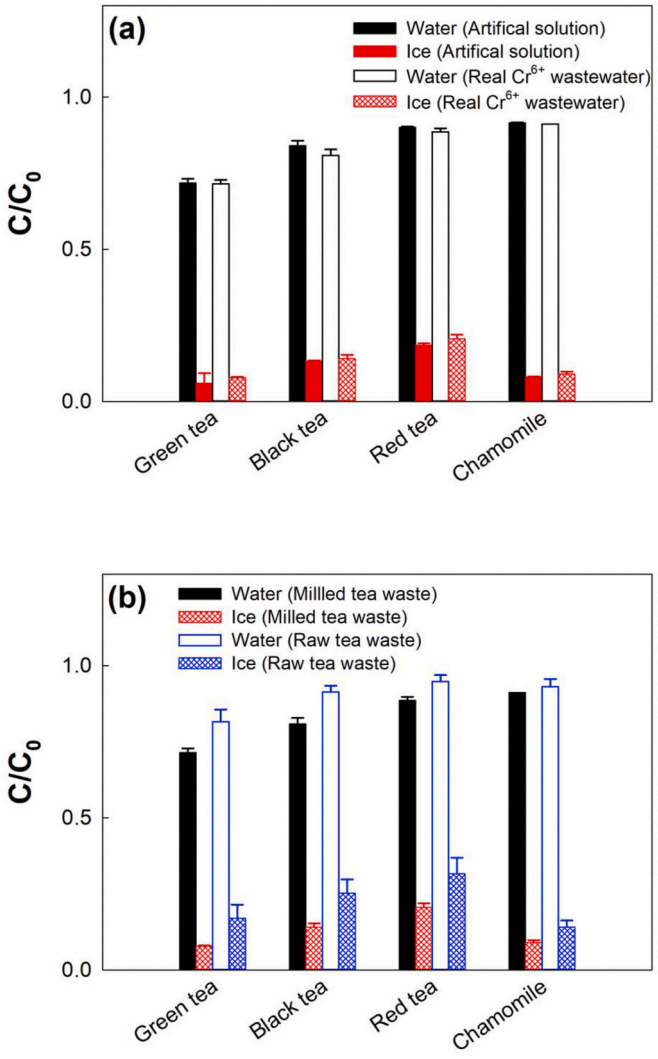

Fig. 9. Reduction of Cr^{6+} in electroplating wastewater. Experimental conditions: $C_0 = [Cr^{6+}]_i = 20$ μM, [tea waste] = 0.1 g/L, $pH_i = 3.5$, reaction time = 5 h, and freezing temperature = −20 °C.

Acknowledgement

This research was supported by the Korea Polar Research Institute (KOPRI) project (PE21120), and was a part of the project titled, "Development of potential antibiotic compounds using polar organism resources (15250103, KOPRI Grant PM20030)." funded by the Ministry of Oceans and Fisheries, Korea.

Appendix A. Supplementary data

Supplementary data to this article can be found online at https://doi.org/10.1016/j.envres.2021.111059.

Author statement

Tae Uk Han: Investigation, Writing - Original Draft. Jungwon Kim: Writing - Review & Editing, Kitae Kim: Conceptualization, Writing - Review & Editing, Supervision.

Funding sources

This research was supported by the Korea Polar Research Institute (KOPRI) project (PE21120), and was a part of the project titled, "Development of potential antibiotic compounds using polar organism resources (15250103, KOPRI Grant PM20030)." funded by the Ministry of Oceans and Fisheries, Korea.

References

Akika, F.Z., Benamira, M., Lahmar, H., Trari, M., Avramova, I., Suzer, S., 2020. Structural and optical properties of Cu-doped $ZnAl_2O_4$ and its application as photocatalyst for Cr(VI) reduction under sunlight. Surf. Interfaces 18, 100406. https://doi.org/10.1016/j.surfin.2019.100406.

Archundia, C., Bonato, P.S., Rivera, J.F.L., Mascioli, L.C., Collins, K.E., Collins, C.H., 1993. Reduction of low concentration Cr (VI) in acid solutions. Sci. Total Environ. 130–131, 231–236. https://doi.org/10.1016/0048-9697(93)90077-J.

Cerrato, A., Cannazza, G., Capriotti, A.L., Citti, C., La Barbera, G., Laganà, A., Montone, C.M., Piovesana, S., Cavaliere, C., 2020. A new software-assisted analytical workflow based on high-resolution mass spectrometry for the systematic study of phenolic compounds in complex matrices. Talanta 209, 120573. https://doi.org/10.1016/j.talanta.2019.120573.

Chen, W., Westerhoff, P., Leenheer, J.A., Booksh, K., 2003. Fluorescence excitation−emission matrix regional integration to quantify spectra for dissolved organic matter. Environ. Sci. Technol. 37, 5701–5710. https://doi.org/10.1021/es034354c.

Chen, X., Chen, G., Chen, L., Chen, Y., Lehmann, J., McBride, M.B., Hay, A.G., 2011. Adsorption of copper and zinc by biochars produced from pyrolysis of hardwood and corn straw in aqueous solution. Bioresour. Technol. 102, 8877–8884. https://doi.org/10.1016/j.biortech.2011.06.078.

Cherdchoo, W., Nithettham, S., Charoenpanich, J., 2019. Removal of Cr (VI) from synthetic wastewater by adsorption onto coffee ground and mixed waste tea. Chemosphere 221, 758–767. https://doi.org/10.1016/j.chemosphere.2019.01.100.

Choi, Y., Yoon, H.-I., Lee, C., Vetráková, L., Heger, D., Kim, K., Kim, J., 2018. Activation of periodate by freezing for the degradation of aqueous organic pollutants. Environ. Sci. Technol. 52, 5378–5385. https://doi.org/10.1021/acs.est.8b00281.

Cleverdon, R., Elhalaby, Y., McAlpine, M.D., Gittings, W., Ward, W.E., 2018. Total polyphenol content and antioxidant capacity of tea bags: comparison of black, green, red rooibos, chamomile and peppermint over different steep times. Beverages 4, 15. https://doi.org/10.3390/beverages4010015.

Garg, U.K., Kaur, M.P., Garg, V.K., Sud, D., 2007. Removal of hexavalent chromium from aqueous solution by agricultural waste biomass. J. Hazard Mater. 140, 60–68. https://doi.org/10.1016/j.jhazmat.2006.06.056.

Han, T.U., Kim, J., Kim, K., 2020. Freezing-accelerated removal of chromate by biochar synthesized from waste rice husk. Separ. Purif. Technol. 250, 117233. https://doi.org/10.1016/j.seppur.2020.117233.

Heger, D., Klánová, J., Klán, P., 2006. Enhanced protonation of cresol red in acidic aqueous solutions caused by freezing. J. Phys. Chem. B 110, 1277–1287. https://doi.org/10.1021/jp0553683.

Ju, J., Kim, J., Vetráková, L., Seo, J., Heger, D., Lee, C., Yoon, H.-I., Kim, K., Kim, J., 2017. Accelerated redox reaction between chromate and phenolic pollutants during freezing. J. Hazard Mater. 329, 330–338. https://doi.org/10.1016/j.jhazmat.2017.01.031.

Kim, K., Chung, H.Y., Ju, J., Kim, J., 2017. Freezing-enhanced reduction of chromate by nitrite. Sci. Total Environ. 590–591, 107–113. https://doi.org/10.1016/j.scitotenv.2017.02.176.

Kim, K., Chung, H.Y., Kim, B., Wong, G., Nguyen, A.Q.K., Kim, S., Kim, J., 2020. Freezing-induced simultaneous reduction of chromate and production of molecular iodine: mechanism, kinetics, and practical implications. Environ. Sci. Technol. https://doi.org/10.1021/acs.est.0c05322. Article (in press).

Kim, K., Kim, J., Bokare, A.D., Choi, W., Yoon, H.-I., Kim, J., 2015. Enhanced removal of hexavalent chromium in the presence of H_2O_2 in frozen aqueous solutions. Environ. Sci. Technol. 49, 10937–10944. https://pubs.acs.org/doi/abs/10.1021/acs.est.5b02702.

Lahmar, H., Benamira, M., 2017. Chromate reduction on the novel hetero-system La_2NiO_4/TiO_2 under solar light. In: 2017 Int. Renew. Sustain. Energy Conf. (IRSEC), pp. 1–4. https://doi.org/10.1109/IRSEC.2017.8477244.

Le, N.T.H., Ju, J., Kim, B., Kim, M.S., Lee, C., Kim, S., Choi, W., Kim, K., Kim, J., 2020. Freezing-enhanced non-radical oxidation of organic pollutants by peroxymonosulfate. Chem. Eng. J. 388, 124226. https://doi.org/10.1016/j.cej.2020.124226.

Lee, Y.H., Verwilst, P., Kim, H.S., Ju, J., Kim, J.S., Kim, K., 2019. Enhanced sensitivity of fluorescence-based Fe (II) detection by freezing. Chem. Commun. 55, 12136–12139. https://doi.org/10.1039/C9CC05809E.

Li, H., Dong, X., de Silva, E.B., de Oliveira, L.M., Chen, Y., Ma, L.Q., 2017. Mechanisms of metal sorption by biochars: Biochar characteristics and modifications. Chemosphere 178, 466–478. https://doi.org/10.1016/j.chemosphere.2017.03.072.

Li, W., Ling, C., Dong, L., Zhao, X., Wu, H., 2021. Accumulation and characteristics of fluorescent dissolved organic matter in loess soil-based subsurface wastewater infiltration system with aeration and biochar addition. Environ. Pollut. 269, 116100. https://doi.org/10.1016/j.envpol.2020.116100.

Lin, L.-Z., Chen, P., Harnly, J.M., 2008. New phenolic components and chromatographic profiles of green and fermented teas. J. Agric. Food Chem. 56, 8130–8140. https://doi.org/10.1021/jf800986s.

Lin, L.-Z., Harnly, J.M., 2010. Identification of the phenolic components of chrysanthemum flower (*Chrysanthemum morifolium* Ramat). Food Chem. 120, 319–326. https://doi.org/10.1016/j.foodchem.2009.09.083.

Lin, Y.-S., Tsai, Y.-J., Tsay, J.-S., Lin, J.-K., 2003. Factors affecting the levels of tea polyphenols and caffeine in tea leaves. J. Agric. Food Chem. 51, 1864–1873. https://doi.org/10.1021/jf021066b.

Liu, C., Pujol, D., Olivella, M.À., de la Torre, F., Fiol, N., Poch, J., Villaescusa, I., 2015. The role of exhausted coffee compounds on metal ions sorption. Water Air Soil Pollut. 226, 289. https://doi.org/10.1007/s11270-015-2568-2.

López-García, M., Lodeiro, P., Barriada, J.L., Herrero, R., Sastre de Vicente, M.E., 2010. Reduction of Cr (VI) levels in solution using bracken fern biomass: batch and column studies. Chem. Eng. J. 165, 517–523. https://doi.org/10.1016/j.cej.2010.09.058.

Mystrioti, C., Xanthopoulou, T.D., Tsakiridis, P., Papassiopi, N., Xenidis, A., 2016. Comparative evaluation of five plant extracts and juices for nanoiron synthesis and application for hexavalent chromium reduction. Sci. Total Environ. 539, 105–113. https://doi.org/10.1016/j.scitotenv.2015.08.091.

Nguyen, Q.A., Kim, B., Chung, H.Y., Kim, J., Kim, K., 2020. Enhanced reduction of hexavalent chromium by hydrogen sulfide in frozen solution. Separ. Purif. Technol. 251, 117377. https://doi.org/10.1016/j.seppur.2020.117377.

Nguyen, Q.A., Kim, B., Chung, H.Y., Nguyen, A.Q.K., Kim, J., Kim, K., 2021. Reductive transformation of hexavalent chromium by ferrous ions in a frozen environment: mechanism, kinetics, and environmental implications. Ecotoxicol. Environ. Saf. 208, 111735. https://doi.org/10.1016/j.ecoenv.2020.111735.

O'Concubhair, R., O'Sullivan, D., Sodeau, J.R., 2012. Dark oxidation of dissolved gaseous mercury in polar ice mimics. Environ. Sci. Technol. 46, 4829–4836. https://doi.org/10.1021/es300309n.

Prabhakaran, S.K., Vijayaraghavan, K., Balasubramanian, R., 2009. Removal of Cr (VI) ions by spent tea and coffee dusts: reduction to Cr (III) and biosorption. Ind. Eng. Chem. Res. 48, 2113–2117. https://pubs.acs.org/doi/10.1021/ie801380h.

Sari, F., Velioglu, Y.S., 2011. Effects of particle size, extraction time and temperature, and derivatization time on determination of theanine in tea. J. Food Compos. Anal. 24, 1130–1135. https://doi.org/10.1016/j.jfca.2011.04.003.

Siddiqui, M.Z., Han, T.U., Park, Y.-K., Kim, Y.-M., Kim, S., 2020. Catalytic pyrolysis of Tetra Pak over acidic catalysts. Catalysts 10, 602. https://doi.org/10.3390/catal10060602.

Stander, M.A., Joubert, E., de Beer, D., 2019. Revisiting the caffeine-free status of rooibos and honeybush herbal teas using specific MRM and high-resolution LC-MS methods. J. Food Compos. Anal. 76, 39–43. https://doi.org/10.1016/j.jfca.2018.12.002.

Takenaka, N., Ueda, A., Maeda, Y., 1992. Acceleration of the rate of nitrite oxidation by freezing in aqueous solution. Nature 358, 736–738. https://doi.org/10.1038/358736a0.

Xu, X., Huang, H., Zhang, Y., Xu, Z., Cao, X., 2019. Biochar as both electron donor and electron shuttle for the reduction transformation of Cr (VI) during its sorption. Environ. Pollut. 244, 423–430. https://doi.org/10.1016/j.envpol.2018.10.068.